On the dynamics of the Fermi-Bose model

Magnus Ögren
Nano-Science Center, Copenhagen University.
DTU-Mathematics, Technical University of Denmark.

In collaboration with Marcus Carlsson
Center for Mathematical Sciences, Lund University.

BIT Circus, Copenhagen,
23-24 of August 2012

Abstract

In this article we formulate and prove results for the exponential matrix representing the dynamics of the Fermi-Bose model in an undepleted bosonic field approximation. A recent application of this model is molecular dimers dissociating into its atomic compounds. The problem is solved in D spatial dimensions by dividing the system matrix into blocks with generalizations of Hankel matrices, here refered to as D-block-Hankel matrices. The method is practically useful for treating large systems, i.e. dense computational grids or higher spatial dimensions, either on a single standard computer or a cluster. In particular the results can be used for studies of three-dimensional physical systems of arbitrary geometry. We illustrate the generality of our approach by giving numerical results for the dynamics of Glauber type atomic pair correlation functions for a non-isotropic three-dimensional harmonically trapped molecular Bose-Einstein condensate.

Outline of my talk:

Background: ***What is the problem we would like to say something about using numerical calculations?***
Quantum dynamics of molecular BEC dissociation!

Formulation: ***How can we write up the dynamical evolution of the system in differential equations?***
Linear ODEs for operators, evolve a complex matrix!

Improvements: ***What have we done to be able to treat large (i.e. realistic) arbitrary shaped 3D systems?***
Symmetries for block-matrices, D-block-Hankel matrix!

Some numerical results!

Motivation to study dissociation into fermions:

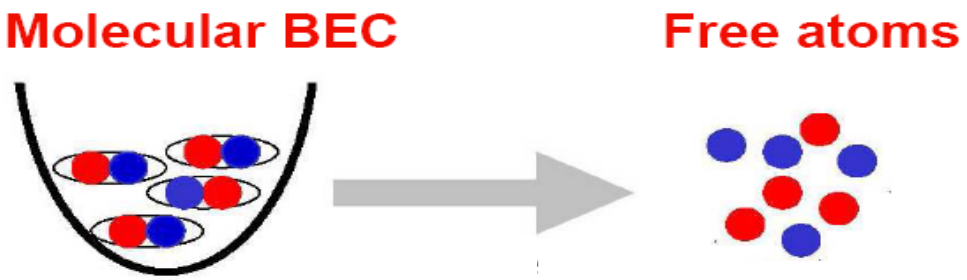

dimers **fermions**

i) Conceptual:

Molecular dissociation as a fermionic analog of optical parametric down-conversion, a good candidate for developing the paradigm of *fermionic quantum atom optics* in fundamental physics and a test bench for simulations.

ii) Pragmatic:

Can we explain the experimentally observed pair-correlations. (Molecules made up of fermions have longer lifetime.)

Fermi-Bose Hamiltonian and applications

$$\hat{H} = \hat{H}_0 - i\hbar\chi \int d\mathbf{x} \left(\hat{\Psi}_0^\dagger \hat{\Psi}_2 \hat{\Psi}_1 - \hat{\Psi}_1^\dagger \hat{\Psi}_2^\dagger \hat{\Psi}_0 \right)$$

1.2 Applications of the Fermi-Bose model

In modern condensed matter physics the Fermi-Bose model have two major areas of applicability. First the so called "s-channel" model in high-temperature superconductivity [1]. In this context it model the formation dynamics of bosonic Cooper-pairs,

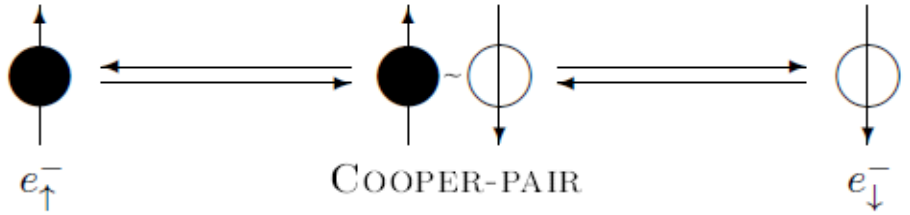

where the two atomic particles, the electrons, are fermions.

In the field of ultra-cold atomic physics, it can model the dissociation of ultra-cold bosonic molecules [13, 14],

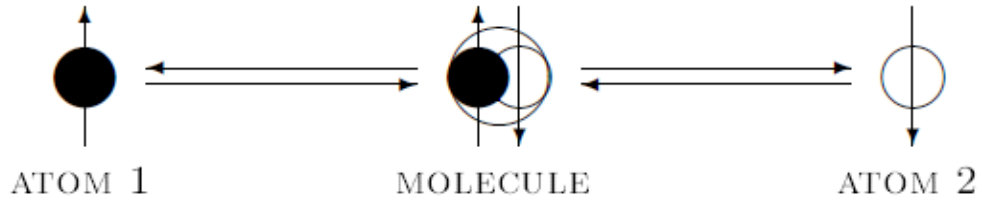

and hence we allow here for the atomic particles to be either two fermions or two bosons.

Exact simulation of molecular dissociation: MÖ, KK, JC, E.P.L. 2010.

We have earlier applied the Gaussian phase-space representation to stochastically model a 1D uniform molecular BEC dissociating into fermionic atoms.

$$\hat{H} = \hbar \sum_{\mathbf{k},\sigma} \Delta_{\mathbf{k}} \hat{n}_{\mathbf{k},\sigma} - i\hbar\kappa_D \sum_{\mathbf{k}} \left(\hat{a}^\dagger \hat{b}_{\uparrow,\mathbf{k}} \hat{b}_{\downarrow,-\mathbf{k}} - \hat{b}^\dagger_{\downarrow,-\mathbf{k}} \hat{b}^\dagger_{\uparrow,\mathbf{k}} \hat{a} \right)$$

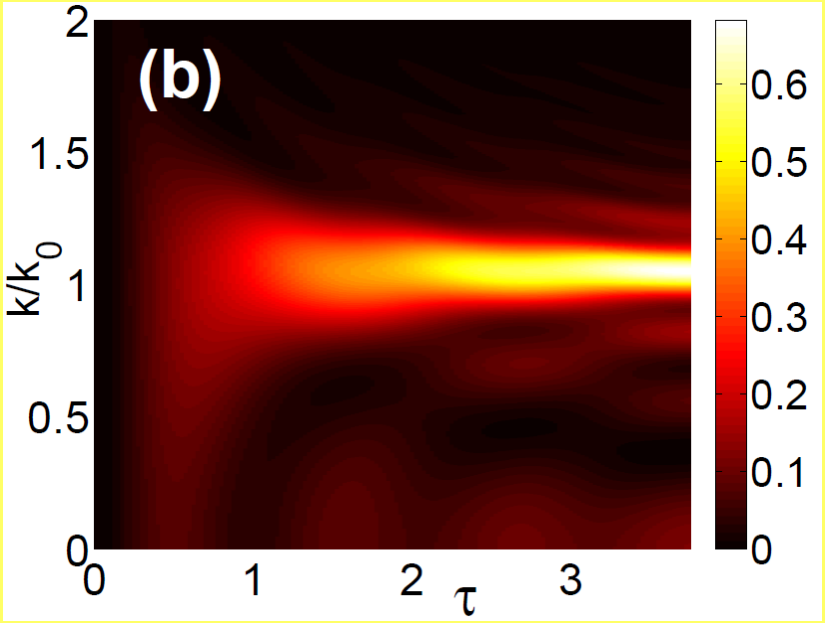

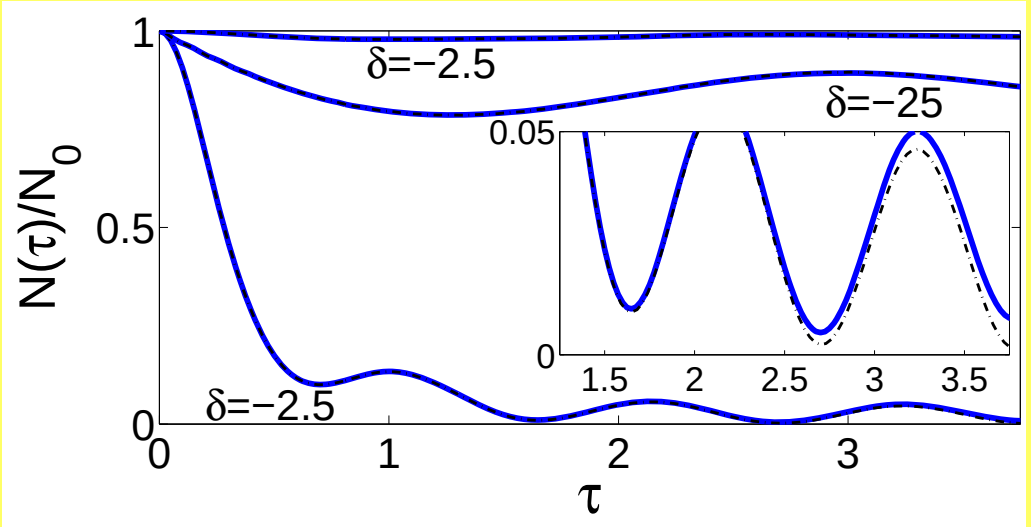

$$t_0 = 1/\kappa\sqrt{N_0}$$

Implement a molecular-field approximation

2.1 Heisenberg equations in the undepleted molecular condensate approximation

From the Heisenberg equation of motion with the Hamiltonian taken from (2), we have for the three field operators

$$\frac{\partial \hat{\Psi}_j(\mathbf{x})}{\partial t} = -\frac{i}{\hbar}\left[\hat{\Psi}_j(\mathbf{x}), \hat{H}\right], \; j = 0,\, 1,\, 2. \tag{3}$$

then replace the molecular field operator by its coherent mean-field complex function, the condensate wavefunction, $\widehat{\Psi}_0(\mathbf{x},t) \rightarrow \langle \widehat{\Psi}_0(\mathbf{x},t)\rangle \equiv \Psi_0(\mathbf{x},0) = \sqrt{\rho_0(\mathbf{x})}\exp(i\theta(\mathbf{x}))$. From (2) and (3) we then write down the Heisenberg equations for the remaining two coupled atomic field operators as follows

$$\frac{\partial \widehat{\Psi}_1(\mathbf{x},t)}{\partial t} = i\left[\frac{\hbar}{2m_a}\nabla^2 - \Omega\right]\widehat{\Psi}_1(\mathbf{x},t) + q\chi\sqrt{\rho_0(\mathbf{x})}\exp(i\theta(\mathbf{x}))\,\widehat{\Psi}_2^{\dagger}(\mathbf{x},t), \tag{4}$$

Linear operator equations!

$$\frac{\partial \widehat{\Psi}_2^{\dagger}(\mathbf{x},t)}{\partial t} = -i\left[\frac{\hbar}{2m_a}\nabla^2 - \Omega\right]\widehat{\Psi}_2^{\dagger}(\mathbf{x},t) + \chi\sqrt{\rho_0(\mathbf{x})}\exp(-i\theta(\mathbf{x}))\,\widehat{\Psi}_1(\mathbf{x},t). \tag{5}$$

The sign given by q in the second term in (4) is $q = -1$ for fermionic and $q = 1$ for bosonic atoms throughout the paper, as a consequence of different operator (anti-) commutator relations. Multiplying (4) and (5) with $L^{-D/2}\exp(-i\mathbf{k}\cdot\mathbf{x})$,

Fourier transformation to momentum-space

operators in momentum space

$$\widehat{a}_{\mathbf{k},j}(t) = \frac{1}{L^{D/2}} \int_V d\mathbf{x}\, \widehat{\Psi}_j(\mathbf{x},t) \exp(-i\mathbf{k}\cdot\mathbf{x}). \tag{6}$$

The operators $\widehat{a}_{\mathbf{k},j}(t)$ satisfy the usual (commutation-) anti-commutation relations $[\widehat{a}_{\mathbf{k},i}, \widehat{a}^\dagger_{\mathbf{k}',j}]_{-q} = \delta_{ij}\delta_{\mathbf{k},\mathbf{k}'}$ and $[\widehat{a}^\dagger_{\mathbf{k},i}, \widehat{a}^\dagger_{\mathbf{k}',j}]_{-q} = [\widehat{a}_{\mathbf{k},i}, \widehat{a}_{\mathbf{k}',j}]_{-q} = 0$ (i.e. for $q = -1$, $[\,,\,]_{+1} \equiv \{\,,\,\}$). Since the effective Hamiltonian corresponding to (4)-(5) is quadratic in the field operators, higher-order moments or expectation values of products of creation and annihilation operators will factorize according to Wick's theorem into products of the normal and anomalous densities $n_{\mathbf{k},\mathbf{k}',j} \equiv \left\langle \widehat{a}^\dagger_{\mathbf{k},j} \widehat{a}_{\mathbf{k}',j} \right\rangle$ and $m_{\mathbf{k},\mathbf{k}'} \equiv \langle \widehat{a}_{\mathbf{k},1} \widehat{a}_{\mathbf{k}',2} \rangle$.

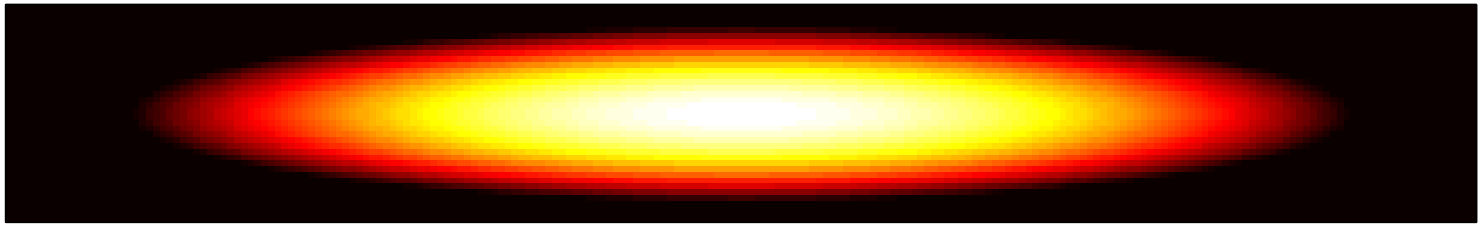

Represent the BEC geometry with a D-dimensional Fourier series.

Linear ODEs for momentum-space operators

$$\frac{d\widehat{a}_{\mathbf{k},1}}{dt} = -i\Delta_{\mathbf{k}}\widehat{a}_{\mathbf{k},1} + q\kappa \sum_{\mathbf{k}'} \tilde{g}_{\mathbf{k}'+\mathbf{k}}\widehat{a}^{\dagger}_{\mathbf{k}',2}, \tag{7}$$

$$\frac{d\widehat{a}^{\dagger}_{\mathbf{k},2}}{dt} = \kappa \sum_{\mathbf{k}'} \tilde{g}^{*}_{\mathbf{k}'+\mathbf{k}}\widehat{a}_{\mathbf{k}',1} + i\Delta_{\mathbf{k}}\widehat{a}^{\dagger}_{\mathbf{k},2}. \tag{8}$$

The kinetic part is $\Delta_{\mathbf{k}} \equiv \Omega + \hbar |\mathbf{k}|^2 / (2m_a)$. The effective atom-molecule coupling constant is $\kappa = \chi / L^{D/2}$ [28]. Finally the complex Fourier coefficients $\tilde{g}_{\mathbf{k}}$ of the condensate wave function describing the molecular meanfield in momentum-space is defined analogue to (6)

$$\tilde{g}_{\mathbf{k}} = \frac{1}{L^{D/2}} \int_V d\mathbf{x} \sqrt{\rho_0(\mathbf{x})} \exp\left(i\theta(\mathbf{x}) - i\mathbf{k}\cdot\mathbf{x}\right), \tag{9}$$

Fourier coefficients are delta spikes for uniform systems.

Uniform (even and real) condensate wavefunction

Under the condition of an uniform molecular field i.e. that do not depend on the spatial coordinates $\Psi_0(\mathbf{x}) = \Psi_0 = \sqrt{\rho_0}$, equations (7)-(8) with initial vacuum states for the atoms have analytical solutions for the normal- and anomalous atomic moments $n_{\mathbf{k},\sigma} \equiv \langle \widehat{n}_{\mathbf{k},\sigma} \rangle \equiv \left\langle \widehat{a}^{\dagger}_{\mathbf{k},1} \widehat{a}_{\mathbf{k},1} \right\rangle = \left\langle \widehat{a}^{\dagger}_{-\mathbf{k},1} \widehat{a}_{-\mathbf{k},1} \right\rangle = \left\langle \widehat{a}^{\dagger}_{\mathbf{k},2} \widehat{a}_{\mathbf{k},2} \right\rangle = \left\langle \widehat{a}^{\dagger}_{-\mathbf{k},2} \widehat{a}_{-\mathbf{k},2} \right\rangle$ respectively $m_{\mathbf{k}} \equiv \langle \widehat{a}_{\mathbf{k},1} \widehat{a}_{-\mathbf{k},2} \rangle = \langle \widehat{a}_{-\mathbf{k},1} \widehat{a}_{\mathbf{k},2} \rangle$. The related (PMFT) complex differential equations with initial conditions $n_{\mathbf{k},\sigma}(0) = m_{\mathbf{k}}(0) = 0$ are [28]

$$\frac{dn_{\mathbf{k},\sigma}}{dt} = 2g_0 \mathrm{Re}\left\{m_{\mathbf{k}}\right\}, \tag{10}$$

$$\frac{dm_{\mathbf{k}}}{dt} = -2i\Delta_{\mathbf{k}} m_{\mathbf{k}} + g_0\left(1 + q2n_{\mathbf{k},\sigma}\right), \tag{11}$$

Connects to alternative formulation “PMFT”, but this require two indices per unknown for non-uniform systems.

Uniform (even and real) condensate wavefunction

where $g_0 \equiv \kappa\tilde{g}_0 = \chi\sqrt{\rho_0}$. The corresponding solutions to (10)-(11), calculated explicitly in section 5.2, are

$$n_{\mathbf{k},\sigma} = \frac{g_0^2}{\Delta_{\mathbf{k}}^2 - qg_0^2} \sin^2\left(\sqrt{\Delta_{\mathbf{k}}^2 - qg_0^2}\, t\right), \tag{12}$$

Valuable with analytic solutions for software tests!

$$m_{\mathbf{k}} = \frac{g_0}{\sqrt{\Delta_{\mathbf{k}}^2 - qg_0^2}} \cos\left(\sqrt{\Delta_{\mathbf{k}}^2 - qg_0^2}\, t\right) \sin\left(\sqrt{\Delta_{\mathbf{k}}^2 - qg_0^2}\, t\right)$$
$$-i\frac{g_0\Delta_{\mathbf{k}}}{\Delta_{\mathbf{k}}^2 - qg_0^2} \sin^2\left(\sqrt{\Delta_{\mathbf{k}}^2 - qg_0^2}\, t\right). \tag{13}$$

Note that for bosons ($q = 1$), e.g., the resonance mode ($\Delta_{\mathbf{k}} \equiv 0$) leads to a Bose-enhancement effect in the atomic occupations, described by $n_{\mathbf{k}_0,\sigma}(t) = \sinh^2(g_0 t)$ which grows exponentially with time. In contrast to this, for fermionic atoms, the atomic occupations undergo sinusoidal oscillations and can be kept to a small fraction of the number of molecules also for large times. As noted in [9] the moments (12) and (13) fulfills the equality

$$|m_{\mathbf{k}}|^2 = n_{\mathbf{k},\sigma}\left(1 + qn_{\mathbf{k},\sigma}\right), \tag{14}$$

for a uniform molecular field.

General formulation for a complex BEC wavefunction

3.1 One-dimensional systems

To set the scene, we first discuss a system in one spatial dimension. For a non-uniform system with $D = 1$, set $B = 2K + 1$ and identify the systems of annihilation operators $\{\hat{a}_{n,1}\}_{-K \leq n \leq K}$ and creation operators $\{\hat{a}^{\dagger}_{n,2}\}_{-K \leq n \leq K}$ with the $2B$ dimensional column vector $\left[\widehat{a}_{-K,1} \ldots \widehat{a}_{K,1} \widehat{a}^{\dagger}_{-K,2} \ldots \widehat{a}^{\dagger}_{K,2}\right]^{T}$. Under this identification, Heisenberg equations (7)-(8) can then be visualized in terms of a $2B \times 2B$-system-matrix A composed of four blocks of $B \times B$-matrices

$$\frac{d}{dt}\begin{bmatrix} \widehat{a}_{-K,1} \\ \vdots \\ \widehat{a}_{K,1} \\ \widehat{a}^{\dagger}_{-K,2} \\ \vdots \\ \widehat{a}^{\dagger}_{K,2} \end{bmatrix} = \begin{bmatrix} A_{11} & A_{12} \\ A_{21} & A_{22} \end{bmatrix} \begin{bmatrix} \widehat{a}_{-K,1} \\ \vdots \\ \widehat{a}_{K,1} \\ \widehat{a}^{\dagger}_{-K,2} \\ \vdots \\ \widehat{a}^{\dagger}_{K,2} \end{bmatrix}. \tag{15}$$

It then follows directly from (8) that the coupling matrices A_{12} and A_{21} become Hankel matrices. A Hankel matrix have the following structure $A_{12}(m,\, n) = A_{12}(m-1,\, n+1)$, i.e. the elements are identical when the sum of the row and column indices are constant [40].

General formulation for a complex BEC wavefunction

3.2 Higher-dimensional systems

For $D > 1$, the summation operator that takes the system of creation operators $\{\hat{a}^\dagger_{\mathbf{k}',2}\}_{\mathbf{k}'}$ to the system of annihilation operators $\{\hat{a}_{\mathbf{k},1}\}_{\mathbf{k}}$ is defined via

$$A_{12,\mathbf{n}}(\{\hat{a}^\dagger_{\mathbf{n}',2}\}_{\mathbf{n}'}) = q\kappa \sum_{n'_1=-K}^{K} \cdots \sum_{n'_D=-K}^{K} \tilde{g}_{n_1+n'_1,\ldots,n_D+n'_D} \hat{a}^\dagger_{n'_1,\ldots,n'_D,2}. \tag{16}$$

We call this a D-dimensional finite Hankel operator. These have been studied e.g. in [41] for $D = 2$. Obviously, there are multiple ways to represent the two systems $\{\hat{a}^\dagger_{\mathbf{k}',2}\}_{\mathbf{k}'}$ and $\{\hat{a}_{\mathbf{k},1}\}_{\mathbf{k}}$ as a $2B^D-$dimensional vector. However, with this

3.2.1 Ordering the lattice

Recall that $B = 2K + 1$. The following function

$$f(n_1, \ldots, n_D) = 1 + \sum_{j=1}^{D} (n_j + K)\, B^{D-j}, \tag{17}$$

is a one-to-one mapping from the D-dimensional lattice $n_1, \ldots, n_D$, $n_j \in \{-K, \ldots, K\}$ to $\{1, \ldots, B^D\}$.

Major 3 steps towards a realistic 3D simulation:

***Theory 1**: Define all necessary physical observables in terms of pairs of raws of the matrixexponential.*
***Numerics 1**: Use efficient software (expokit) for the calculation of only these raws from a sparse (truncated) system matrix.*

***Theory 2**: Prove block-matrix symmetries.*
***Numerics 2**: Find block-matrix symmetries and implement them in the corresponding algorithms.*

***Theory 3**: Define a D-block-Hankel matrix structure.*
***Numerics 3**: Implement algorithm for multiplication between a D-block-Hankel matrix and a vector and incorporate them into efficient matrixexponentiation software (expokit).*

1.st step towards a realistic 3D simulation:

Theory 1: Define all necessary physical observables in terms of pairs of raws of the matrixexponential.

Numerics 1: Use efficient software (expokit) for the calculation of theses raws from a sparse (truncation) system matrix.

What do we need to calculate?

5 Obtaining physical observables

In this section we show how to use the results of the previous section for obtaining physical observables for the atoms. We start from the following general block form of the solution $M = \exp(At)$ to Heisenberg equations (7)-(8) in matrix form (20)

$$\begin{bmatrix} \widehat{a}_{1,1}(t) \\ \vdots \\ \widehat{a}_{B^D,1}(t) \\ \widehat{a}^{\dagger}_{1,2}(t) \\ \vdots \\ \widehat{a}^{\dagger}_{B^D,2}(t) \end{bmatrix} = \begin{bmatrix} M_{11} & qM_{12} \\ M_{21} & M_{22} \end{bmatrix} \begin{bmatrix} \widehat{a}_{1,1}(0) \\ \vdots \\ \widehat{a}_{B^D,1}(0) \\ \widehat{a}^{\dagger}_{1,2}(0) \\ \vdots \\ \widehat{a}^{\dagger}_{B^D,2}(0) \end{bmatrix}, \tag{51}$$

It is obvious that the results of the previous section will simplify the practical calculations of $M(t)$ and hence the physical observables. However, first we show in the next section how to generally obtain first-order moments for pairs of atomic operators directly from (51).

Physical observables are formed by pairs of raws

As a first example, for an annihilation operator of the $\sigma = 1$ spin-state in row m in the left hand side of (51) we have

$$\widehat{a}_{m,1}(t) \equiv \widehat{a}_{\mathbf{k},1}(t) = M_{11,\mathbf{k}}\hat{u} + qM_{12,\mathbf{k}}\hat{v} = \hat{u}^T M_{11,\mathbf{k}}^T + q\hat{v}^T M_{12,\mathbf{k}}^T, \tag{52}$$

where we for notational and computational convenience introduce the two operators

$$\hat{u} \equiv \begin{bmatrix} \widehat{a}_{1,1}(0) \\ \vdots \\ \widehat{a}_{B^D,1}(0) \end{bmatrix}, \quad \hat{v} \equiv \begin{bmatrix} \widehat{a}_{1,2}^{\dagger}(0) \\ \vdots \\ \widehat{a}_{B^D,2}^{\dagger}(0) \end{bmatrix},$$

$$m_{\mathbf{k},\mathbf{k}'} \equiv \langle \widehat{a}_{\mathbf{k},1}\widehat{a}_{\mathbf{k}',2} \rangle = \left\langle (M_{11,\mathbf{k}}\hat{u} + qM_{12,\mathbf{k}}\hat{v}) \left(\hat{u}^{\dagger} M_{21,\mathbf{k}'}^{\dagger} + \hat{v}^{\dagger} M_{22,\mathbf{k}'}^{\dagger} \right) \right\rangle$$

$$= \Big\langle M_{11,\mathbf{k}}\hat{u}\hat{u}^{\dagger} M_{21,\mathbf{k}'}^{\dagger} + qM_{12,\mathbf{k}}\hat{v}\hat{u}^{\dagger} M_{21,\mathbf{k}'}^{\dagger}$$

$$+ M_{11,\mathbf{k}}\hat{u}\hat{v}^{\dagger} M_{22,\mathbf{k}'}^{\dagger} + qM_{12,\mathbf{k}}\hat{v}\hat{v}^{\dagger} M_{22,\mathbf{k}'}^{\dagger} \Big\rangle$$

$$= M_{11,\mathbf{k}} \langle \hat{u}\hat{u}^{\dagger} \rangle M_{21,\mathbf{k}'}^{\dagger} + qM_{12,\mathbf{k}} \langle \hat{v}\hat{u}^{\dagger} \rangle M_{21,\mathbf{k}'}^{\dagger}$$

$$+ M_{11,\mathbf{k}} \langle \hat{u}\hat{v}^{\dagger} \rangle M_{22,\mathbf{k}'}^{\dagger} + qM_{12,\mathbf{k}} \langle \hat{v}\hat{v}^{\dagger} \rangle M_{22,\mathbf{k}'}^{\dagger} = M_{11,\mathbf{k}} M_{21,\mathbf{k}'}^{\dagger}, \tag{54}$$

which is a time-dependent complex number as expected.

Any observable is available (Wick approximated)

5.3 Higher-order atomic moments

Higher-order moments, such as in the simplest case, the combination of two pairs of operators, are factorized according to Wick's theorem [33] which is implicit from the decorrelation assumption in use within the undepleted molecular field approximation here. As an example we calculate Glauber's correlation function for two atoms in the same spin-state [23]

$$g^{(2)}_{\sigma\sigma}\left(\mathbf{k},\mathbf{k}',t\right) \equiv \frac{\left\langle \widehat{a}^{\dagger}_{\mathbf{k},\sigma}\widehat{a}^{\dagger}_{\mathbf{k}',\sigma}\widehat{a}_{\mathbf{k}',\sigma}\widehat{a}_{\mathbf{k},\sigma}\right\rangle}{n_{\mathbf{k},\sigma}n_{\mathbf{k}',\sigma}} = 1 + \frac{q\left|n_{\mathbf{k},\mathbf{k}',\sigma}\right|^{2}}{n_{\mathbf{k},\mathbf{k},\sigma}n_{\mathbf{k}',\mathbf{k}',\sigma}}. \tag{65}$$

For a numerical implementation of (65) we have, according to (58),

$$g^{(2)}_{\sigma\sigma}\left(\mathbf{k},\mathbf{k}',t\right) = 1 + \frac{q\left|M^{*}_{12,\mathbf{k}}M^{T}_{12,\mathbf{k}'}\right|^{2}}{\left(M^{*}_{12,\mathbf{k}}M^{T}_{12,\mathbf{k}}\right)\left(M^{*}_{12,\mathbf{k}'}M^{T}_{12,\mathbf{k}'}\right)}. \tag{66}$$

2.nd step towards a realistic 3D simulation:

Theory 2: Prove block-matrix symmetries.

Numerics 2: Find block-matrix symmetries and implement them in the corresponding algorithms.

General formulation for a complex BEC wavefunction

matrices. In the coming two sections we discuss properties of the four block matrices A_{11}, A_{12}, A_{21} and A_{22}.

We will use the following notation; T denotes transpose, $*$ is complex conjugation, and $\dagger$ represents both the two previous operations combined. Moreover, the operation of transposing in the skew-diagonal will be denoted SDT, i.e.

$$A^{SDT}(m^R, m^C) = A(B^D + 1 - m^C, B^D + 1 - m^R), \tag{21}$$

or equivalently

$$A^{SDT} = \mathbb{S}A^T\mathbb{S}, \tag{22}$$

where $\mathbb{S}$ denotes the skew-diagonal identity, i.e. the matrix obtained by reversing the order of the columns of the identity matrix $\mathbb{I}$. From (22) and the property $\mathbb{S}\mathbb{S} = \mathbb{I}$, it also follow that the skew-diagonal transpose of the product of two general matrices B_1 and B_2 fulfills

$$(B_1B_2)^{SDT} = B_2^{SDT}B_1^{SDT}, \tag{23}$$

which will be used later.

Finally, the skew-diagonal transpose combined with complex conjugation will be denoted SDH.

Real and even BEC wavefunctions

remainder. First we note that

$$A_{12}^{T} = A_{12}, \tag{28}$$

which is immediate by (24).

To get additional structure, we impose extra conditions on the condensate wave-function $\Psi = \sqrt{\rho(\mathbf{x})}\exp(i\theta(\mathbf{x}))$. For many physical applications, $\Psi = \sqrt{\rho(\mathbf{x})}$ can be chosen real. In this case, we note that the Fourier coefficients (9) have the following symmetry $\tilde{g}_{-n_1^F,\ldots,-n_D^F} = \tilde{g}^*_{n_1^F,\ldots,n_D^F}$. Therefore we get from (19)

$$A_{12}^{SDH} = A_{12}, \tag{29}$$

and from (27) that

$$A_{21} = qA_{12}^{SDT}. \tag{30}$$

Furthermore, for the physically important case of a condensate wave-function that is real and even, i.e. with $\rho(\mathbf{x}) = \rho(-\mathbf{x})$, such as for example for a condensate in a harmonic trap, we have that $\tilde{g}_{\mathbf{n}}$ is real so $A_{12}^* = A_{12}$, which combined with (29) implies that

$$A_{12}^{SDT} = A_{12}, \tag{31}$$

and from (27) that

$$A_{21} = qA_{12}. \tag{32}$$

Finally, we perform a trivial check of that the real ($\theta = 0$) uniform (even) case $\rho(\mathbf{x}) = \rho_0$ inserted into (9) gives a real non-zero $\tilde{g}_{\mathbf{k}} = \tilde{g}_0$ only at positions where $(n_1^R,\ldots,n_D^R) = -(n_1^C,\ldots,n_D^C)$, i.e., $A_{12} = qA_{21} = q\kappa\tilde{g}_0\mathbb{S}$. It is important to note that for this special case we have the results of section 2.2.

3.3.2 Diagonal matrices for the kinetic energy

From symmetries in the system matrix to the observables

4 On the block-structure of the propagator

Much of the structure of the system-matrix A is preserved in matrix functions defined on A, which can be used to reduce the computational complexity when evaluating $\exp(At)$ for the system's evolution in time. Naturally, the more conditions we impose on the condensate wave-function Ψ in (9), the more structure is preserved. We present the corresponding identities in order of increasing symmetry on Ψ, starting with a general complex condensate wave-function. Throughout we will let $q = \pm 1$ and prove the results for the cases of fermionic ($q = -1$) and bosonic ($q = 1$) atoms simultaneously.

Given an arbitrary square (even sized) $2n \times 2n$-matrix B we decompose it into its four blocks

$$B = \begin{bmatrix} B_{11} & B_{12} \\ B_{21} & B_{22} \end{bmatrix}.$$

Below we list a number of useful matrix identities which all can be verified by direct computation

$$\begin{bmatrix} 0 & q\mathbb{I} \\ \mathbb{I} & 0 \end{bmatrix} \begin{bmatrix} B_{11} & B_{12} \\ B_{21} & B_{22} \end{bmatrix} \begin{bmatrix} 0 & \mathbb{I} \\ q\mathbb{I} & 0 \end{bmatrix} = \begin{bmatrix} B_{22} & qB_{21} \\ qB_{12} & B_{11} \end{bmatrix}, \tag{36}$$

$$\begin{bmatrix} B_{11} & B_{12} \\ B_{21} & B_{22} \end{bmatrix}^{\dagger} = \begin{bmatrix} B_{11}^{\dagger} & B_{21}^{\dagger} \\ B_{12}^{\dagger} & B_{22}^{\dagger} \end{bmatrix}, \tag{37}$$

$$\begin{bmatrix} B_{11} & B_{12} \\ B_{21} & B_{22} \end{bmatrix}^{SDT} = \begin{bmatrix} B_{22}^{SDT} & B_{12}^{SDT} \\ B_{21}^{SDT} & B_{11}^{SDT} \end{bmatrix}. \tag{38}$$

With these three identities at hand, the following lemmas are all immediate. For example the first one is a direct application of (36) alone.

From symmetries in the system matrix to the propagator

4.1 Lemma

The matrix identities

$$B_{11} = B_{22}^*, \; B_{12} = qB_{21}^*, \tag{39}$$

are equivalent to

$$B = \begin{bmatrix} 0 & q\mathbb{I} \\ \mathbb{I} & 0 \end{bmatrix} B^* \begin{bmatrix} 0 & \mathbb{I} \\ q\mathbb{I} & 0 \end{bmatrix}. \tag{40}$$

The second lemma follows by combining (36) with (38).

4.2 Lemma

4.3 Lemma

4.4 Proposition

Let B be the system-matrix A constructed in section 3.3 from the condensate wave-function Ψ. Then the identities in (39) of Lemma 4.1 are always satisfied. Moreover, if Ψ is real then the identities in (41) of Lemma 4.2 hold and if Ψ is real and even, the identities in (43) of Lemma 4.3 hold.

Proof. The first claim follows by combining (27) and (34), and the second follows by combining (30) and (35). When Ψ is also even the elements of A_{12} are real, and hence (28) can be written $A_{12}^\dagger = A_{12}$ (analogously $A_{21}^\dagger = A_{21}$). Since clearly $A_{11} = A_{22}^\dagger$, the last claim is established as well.

□

From symmetries in the system matrix to the propagator

4.5 Theorem

Let $\phi(z) = \sum_{k=0}^{\infty} c_k z^k$ be an entire function and let A be a matrix that satisfies either of the identities in (39), (41) or (43). Then $\phi(A)$ satisfies the same identities.

Proof. Let us suppose that A satisfies the identities of (41). By Lemma 4.2 we then have (42), which combined with (23) and (45), yields that

$$A^k = \begin{bmatrix} 0 & q\mathbb{I} \\ \mathbb{I} & 0 \end{bmatrix} (A^k)^{SDT} \begin{bmatrix} 0 & \mathbb{I} \\ q\mathbb{I} & 0 \end{bmatrix},$$

for any k. Thus the matrix identities in (41) are satisfied for the corresponding blocks of $M = \phi(A)$ when ϕ is a monomial. Since (41) are also preserved upon taking linear combinations of matrices that all satisfy (41), we conclude that (41) holds whenever ϕ is a polynomial. Finally, since in the general case we have

$$\phi(A) = \lim_{N\to\infty} \sum_{k=0}^{N} c_k A^k,$$

in the operator norm, and since the identities (41) are preserved upon taking limits with respect to this norm [see (46)], the general result follows. The proofs related to (39) and (43) are analogue.

□

Real BEC wavefunction

4.6 Corollary

Given a real condensate wave-function Ψ *and* $t \in \mathbb{R}$, *set*

$$M = \exp(At) \equiv \sum_{j=0}^{\infty} \frac{(At)^j}{j!}. \tag{47}$$

Then M *has the structure*

$$M = \begin{bmatrix} M_{11} & qM_{12} \\ M_{12}^* & M_{11}^* \end{bmatrix}, \tag{48}$$

where in addition we have for the two blocks

$$M_{11}^{SDT} = M_{11},\ M_{12}^{SDH} = M_{12}. \tag{49}$$

Proof. We can see that M has the above structure if and only if it satisfies the identities in (39) and (41) of Lemmas 4.1 and 4.2. Moreover, A satisfies these identities by Proposition 4.4. The desired conclusion thus follows by Theorem 4.5.

□

Real and even BEC wavefunction (common in exp.)

4.7 Corollary

Suppose that Ψ is a real and even condensate wave-function. Then, in addition to the identities in Corollary 4.6, we have

$$M_{11}^T = M_{11},\ M_{12}^\dagger = M_{12}. \tag{50}$$

Proof. By Proposition 4.4 A satisfies the identities in (43) of Lemma 4.3, and hence so does M by Theorem 4.5. It is easy to see that these identities combined with the structure in (48) and (49) proven in Corollary 4.6 implies that the above identities are satisfied for M .

□

From Corollary 4.7 follows that we only need to calculate a quarter of the matrices M_{11} and M_{12} in order to fully determine M, which further reduces the computational cost to $2\left(n^2/4\right) = n^2/2$ elements in this case.

3.rd step towards a realistic 3D simulation:

Theory 3: Define a D-block-Hankel matrix structure.

Numerics 3: Implement algorithm for multiplication between a D-block-Hankel matrix and a vector and incorporate them into efficient matrixexponentiation software (expokit).

General formulation for a complex BEC wavefunction

3.3.1 Structure of the D-block-Hankel matrices

Inspection of (7)-(8) and (20) shows that A_{12} is given elementwise by

$$A_{12}\left(m^R, m^C\right) = q\kappa\tilde{g}_{f^{-1}(m^R)+f^{-1}(m^C)}. \tag{24}$$

Note that the relation between integer coordinates n_j^F for the Fourier coefficients and the coordinates for the rows and columns fulfills

$$\begin{cases} n_1^F = n_1^R + n_1^C \\ \vdots \\ n_D^F = n_D^R + n_D^C \end{cases}, \tag{25}$$

which considerably simplify any practical implementation of A_{12}. Note also that when $\tilde{g}_{\mathbf{k}}$ is defined on the same $\mathbf{k}$-lattice as the atomic operators, we necessarily have $\tilde{g}_{\mathbf{k}} \equiv 0$ when $\left|n_j^R + n_j^C\right| > K$, see figure 1 for an illustration.

Similarly to (24), we have

$$A_{21}\left(m^R, m^C\right) = \kappa\tilde{g}^*_{f^{-1}(m^R)+f^{-1}(m^C)}, \tag{26}$$

such that $(q^2 = 1)$

$$A_{21} = qA_{12}^*. \tag{27}$$

Visualization of a D-block-Hankel matrix (D=3, K=30)

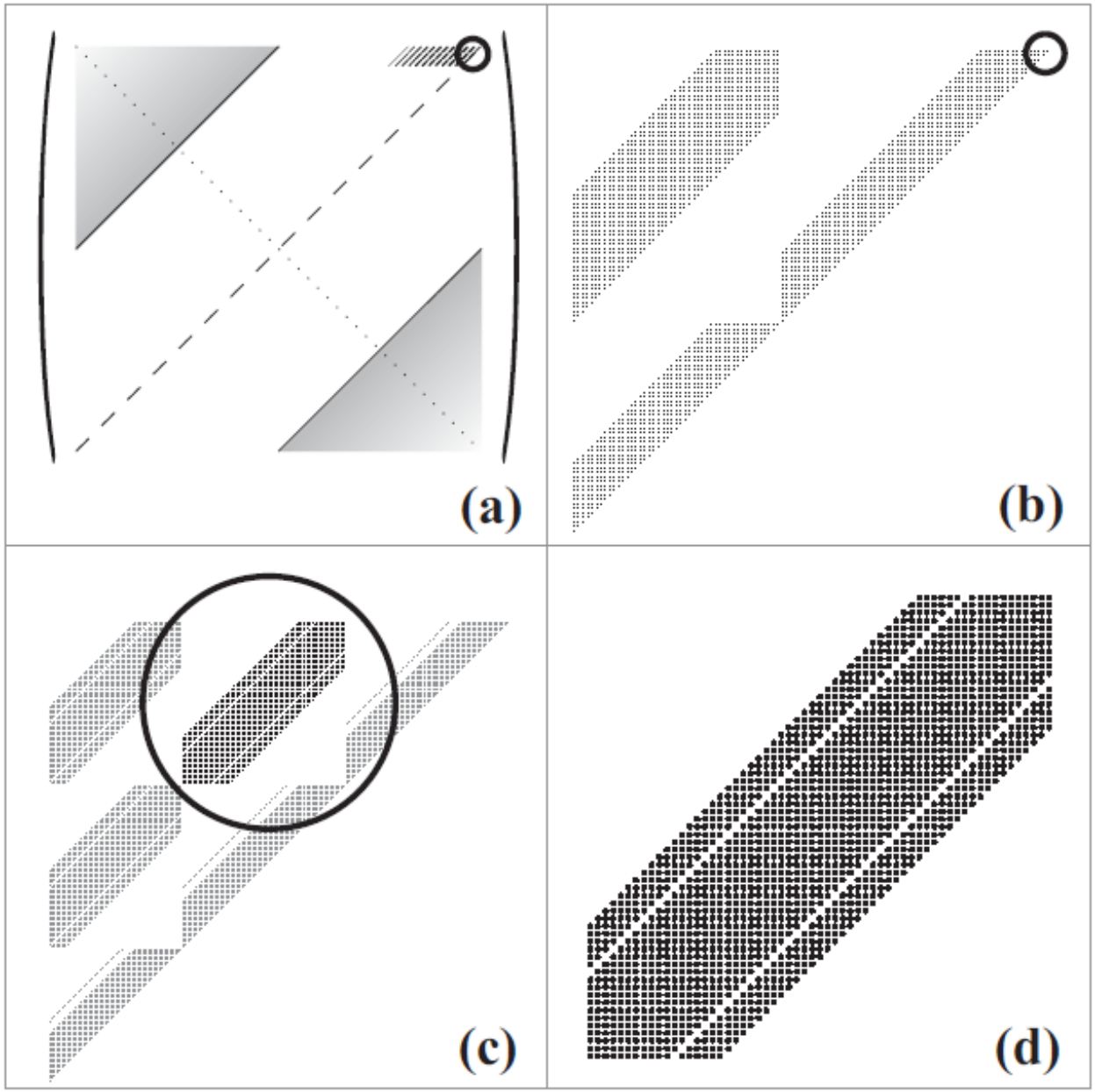

Visualization of a D-block-Hankel matrix (D=3, K=30)

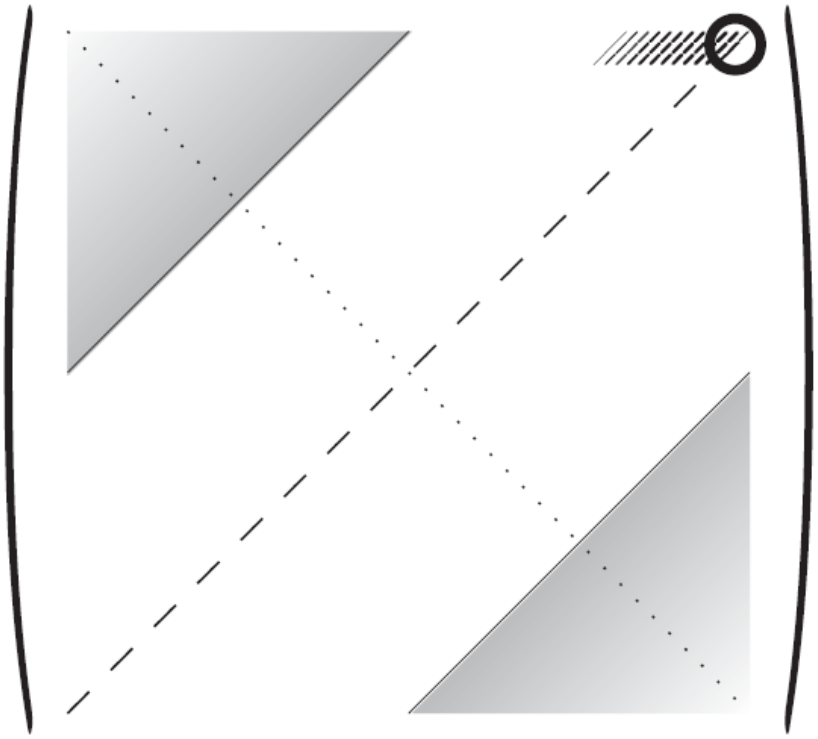

(a)

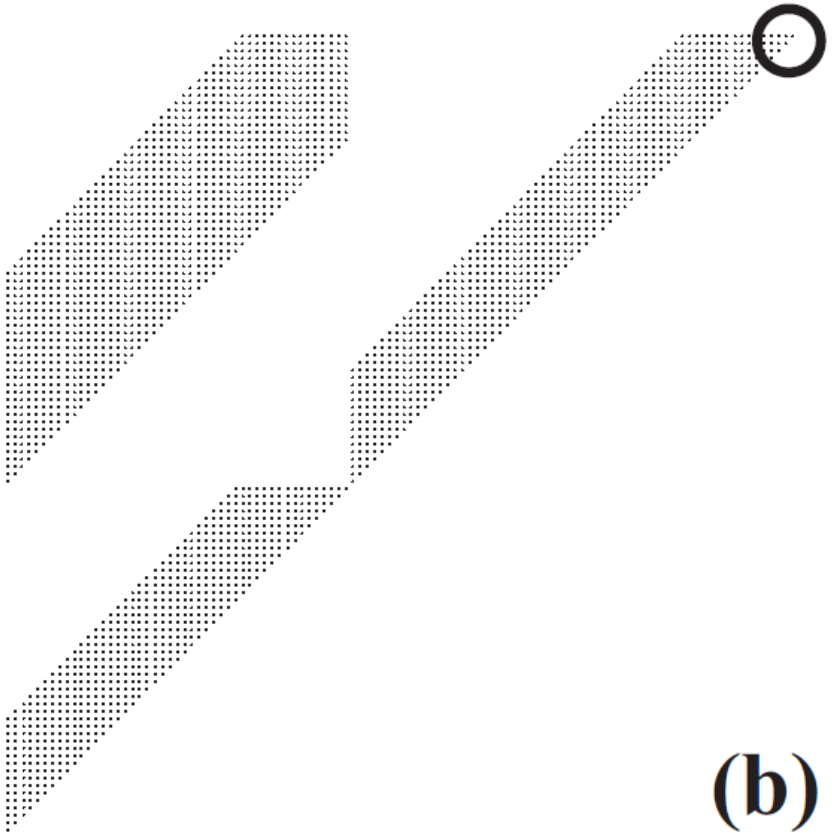

(b)

Visualization of a D-block-Hankel matrix (D=3, K=30)

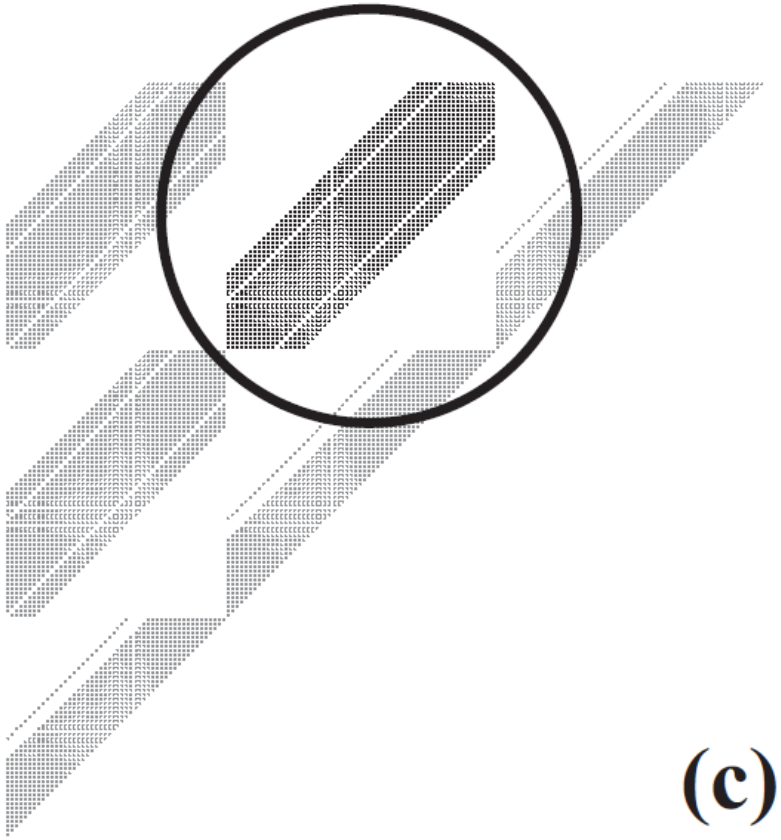

(c)

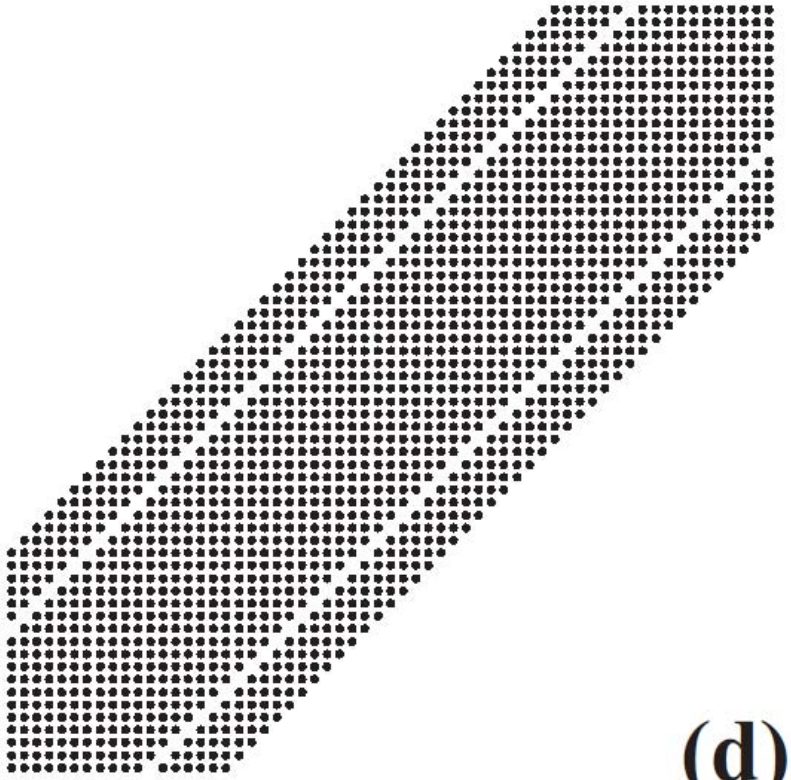

(d)

Numerical results for fermionic atom-atom correlations

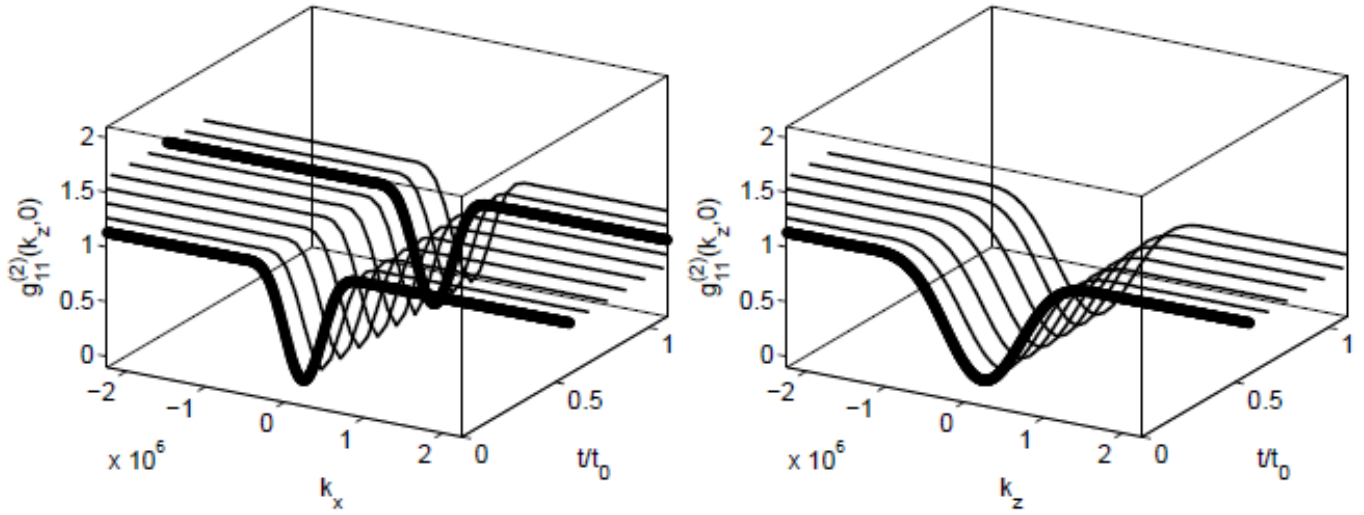

Figure 2: Fermionic collinear atom-atom correlation functions in momentum space $g^{(2)}_{11}(\mathbf{k},\mathbf{k}',t)$, at times $t/t_0 = 0.1,\ 0.2,\ ...,\ 1$ ($t_0 = 1\text{ms}$), calculated along different directions in 3D. In (a) we show numerical results (solid thin curves) from (66) along the direction $\mathbf{e}_x$, i.e. with $\mathbf{k} = k_x\mathbf{e}_x$ and $\mathbf{k}' = k_0\mathbf{e}_x$ ($k_0 \simeq 2.2 \cdot 10^6\text{m}^{-1}$), while in (b) we show the corresponding result along the direction $\mathbf{e}_z$. Analytic results of (71) are represented by the fat curves plotted at $t/t_0 = 0.1$ only. In general the fermionic collinear correlations are here showing a Pauli-blocking dip at $k_{x,z} = k_0$, while the characteristic width of the correlation signal have been confirmed to be inversely proportional to the size of the molecular BEC source along the corresponding direction, i.e. $\sim 2.16R^{-1}_{TF,x} \simeq 2.7 \cdot 10^5\text{m}^{-1}$ in (a) and $\sim 2.16R^{-1}_{TF,z} = 2 \cdot 2.16R^{-1}_{TF,x}$ in (b). In addition we compared with the corresponding results for bosonic atoms showing a so called Hanbury-Brown and Twiss peak at $k_{x,z} = k_0$ (dashed curves, shown only for the largest time here).

Numerical evaluations of analytic asymptotes

6.3 Comparison with analytic short-time asymptotes

For $D = 3$ the Thomas-Fermi (TF) density profile of the BEC is given by $\rho_0(\mathbf{x}) = \rho_0(1-x^2/R_{\mathrm{TF},x}^2-y^2/R_{\mathrm{TF},y}^2-z^2/R_{\mathrm{TF},z}^2)$ for $x^2/R_{\mathrm{TF},x}^2+y^2/R_{\mathrm{TF},y}^2+z^2/R_{\mathrm{TF},z}^2 < 1$ [and $\rho_0(\mathbf{x}) = 0$ otherwise], which is underlying the analytic derivation of the asymptotes. Here $R_{\mathrm{TF},i}$ is the Thomas-Fermi radius along the spatial direction $i = x, y, z$. We are here interested in back-to-back (BB) and collinear (CL) density correlations between two momentum components at $\mathbf{k}$ and $\mathbf{k}'$, for which the displacement $\Delta\mathbf{k} = \mathbf{k} - \mathbf{k}'$ is along one of the Cartesian coordinates, k_i, where $i = x, y, z$. The detailed derivation of short-time asymptotes for the correlation functions in this case was reported in [23]. The BB and CL correlations following from these derivations are

$$g_{12}^{(2)}(k_i, k_i', t) \simeq 1 + \frac{225\pi^2}{16t^2\chi^2\rho_0}\frac{\left[J_2\left((k_i + k_i')R_{\mathrm{TF},i}\right)\right]^2}{\left[(k_i + k_i')R_{\mathrm{TF},i}\right]^4}, \tag{70}$$

$$g_{jj}^{(2)}(k_i, k_i', t) \simeq 1 + q\frac{225\pi}{2}\frac{\left[J_{5/2}\left((k_i - k_i')R_{\mathrm{TF},i}\right)\right]^2}{\left[(k_i - k_i')R_{\mathrm{TF},i}\right]^5}. \tag{71}$$

Here J_ν denotes Bessel functions of the first kind. The qualitative behavior of

Collinear (CL) correlations, molecular dissociation

(b) Collinear (CL) correlations due to particle statistics, (like Hanbury Brown and Twiss for photons).

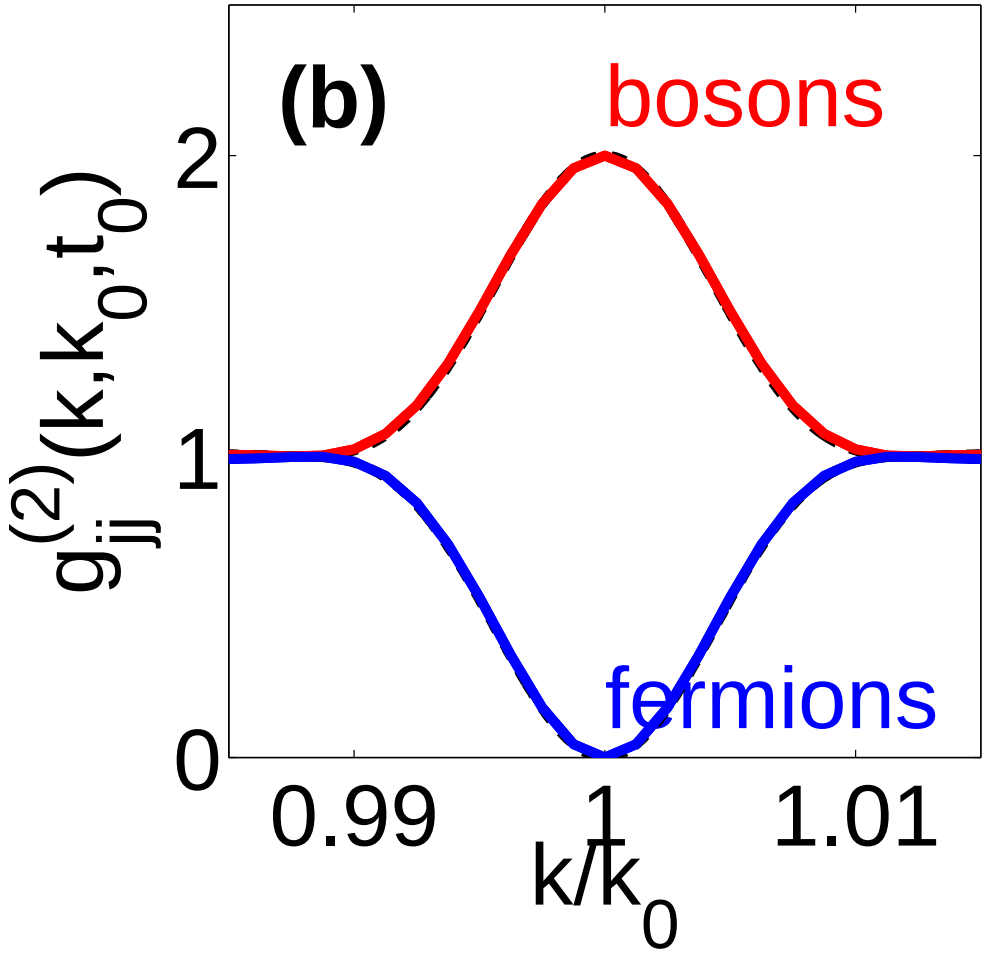

We have derived an analytical asymptote (dashed lines), strictly valid for short times ($t/t_0 \ll 1$). But useful even for $t/t_0 \sim 1$ as here. Solid lines are from a numerical calculation at $t/t_0 = 0.5$.

$$g^{(2)}_{jj}(k,k',t) \simeq 1 \begin{matrix} + \\ - \end{matrix} \frac{9\pi}{2} \frac{\left(J_{3/2}\left[(k-k')R_{\mathrm{TF}}\right]\right)^2}{\left[(k-k')R_{\mathrm{TF}}\right]^3}$$

Observations from the field of ultra-cold atoms:

Bosons

(CL) $g_{j,j}^{(2)}(k,k',t)$, j=1,2

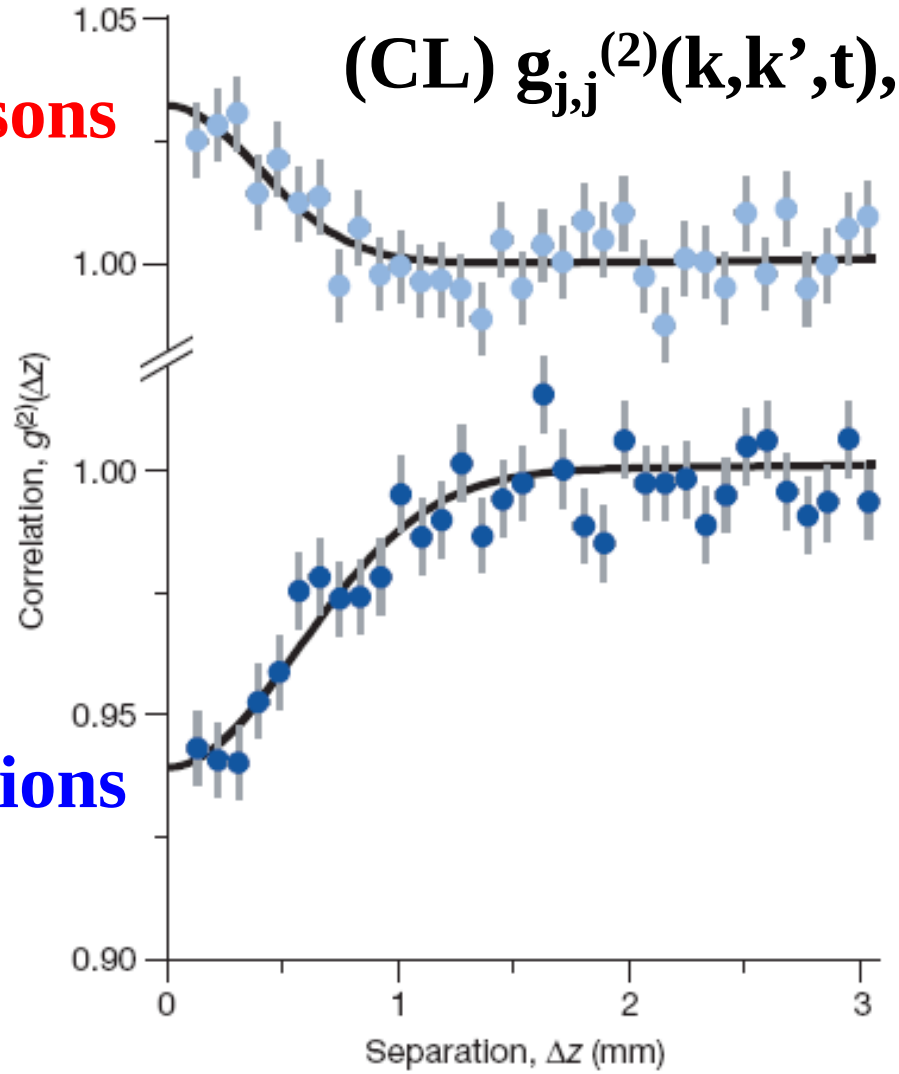

Fermions

Figure 2 | Normalized correlation functions for ^{4}He* (bosons) in the upper plot, and ^{3}He* (fermions) in the lower plot. Both functions are measured at the same cloud temperature (0.5 μK), and with identical trap parameters.

T. Jeltes *et al.*, Nature 445 (2007) 402.

See also: M. Henny *et al.*, Science 284, 296 (1999). For 'anti-bunching of electrons' in a solid state device.

First 3D calculation for general BEC wavefunction

7 Summary

We have described how to effectivelly calculate the dynamics of linear Heisenberg operator equations for the Fermi-Bose model applied to the problem of molecular dissociation. We note that a similar framework have been used to obtain numerical results for a non-isotropic 2D system on a 61×61 grid in [34]. We have here generalized the approch to D spatial dimensions with the use of D-block-Hankel matrices. In particular we have explicitly explored a non-isotropic 3D system on a $61 \times 61 \times 61$ grid numerically on a standard PC. Such a grid can resolve relevant atom dynamics in momentum space for realistic parameters [9], and naturally extends earlier studies of non-uniform 1D and 2D systems [34, 45], and is more realistic than previous treatments of uniform 3D systems [9, 28]. We finally stress that the results presented can be used to handle a complex bosonic mean-field of any geometry in any spatial dimension.

Acknowledgments

We thank Karén Kheruntsyan and Roger Sidje for valuable discussions at an early stage, and Johnny Kvistholm for artistic assistance with figure 1.

Related work:

On the dynamics of the Fermi-Bose model.
M. Ögren and M. Carlsson, To be submitted to J. Phys. A: Math. Gen. 2012.

Stochastic simulations of fermionic dynamics with phase-space representations.
M. Ögren, K. V. Kheruntsyan and J. F. Corney, Comp. Phys. Comm. **182** 1999 (2011).

First-principles quantum dynamics for fermions: application to molecular dissociation.
M. Ögren, K. V. Kheruntsyan and J. F. Corney, Europhys. Lett. **92**, (2010) 36003.

Role of spatial inhomogeneity in dissociation of trapped molecular condensates.
M. Ögren and K. V. Kheruntsyan, Phys. Rev. A **82**, 013641 (2010).

Directional effects due to quantum statistics in dissociation of elongated molecular condensates.
M. Ögren, C. M. Savage and K. V. Kheruntsyan, Phys. Rev. A **79**, 043624 (2009).

Atom-atom correlations from condensate collisions.
M. Ögren and K. V. Kheruntsyan, Phys. Rev. A **79**, 021606(R) (2009).

Atom-atom correlations and relative number squeezing in dissociation of spatially inhomogeneous molecular condensates.
M. Ögren and K. V. Kheruntsyan, Phys. Rev. A **78**, 011602(R) (2008).